2011 American Control Conference
on O'Farrell Street, San Francisco, CA, USA
June 29 - July 01, 2011

Optimal energy management of hybrid electric vehicles including battery aging

Lorenzo Serrao, Simona Onori, Antonio Sciarretta, Yann Guezennec, Giorgio Rizzoni

Abstract— **The paper presents a methodology to account for battery aging in the energy management strategy for a hybrid electric vehicle. An optimal control problem is formulated to minimize fuel consumption as well as battery aging, using recently developed methods for battery lifetime modeling. The approach relies on the concept of severity factor map, a tool used to quantify the aging effects of a battery due to its different on-vehicle operating conditions. The optimal control problem is solved using Pontryagin's Minimum Principle, showing with simulations the effect of the new control approach compared to the standard energy management strategies.**

I. Introduction

Energy management of hybrid electric vehicles [1] is a theme that has seen the contribution of many authors in recent years, with application of traditional optimal control theory, in particular Pontryagin's Minimum Principle, in order to find the solution that is optimal with respect to a given cost function. In most cases, the cost function is the fuel consumption during a driving cycle or the total emissions of carbon dioxide.

In this paper, instead, the optimization objective is the minimization of fuel consumption and battery wear (or aging) during a driving cycle. The overall reduction of battery life deriving from its usage is treated as an additional cost, that can be quantified thanks to an appropriate description of the aging process. The approach leverages recent advances in understanding and quantifying battery aging, summarized in Section II. The optimal control problem is formulated in Section III, and its solution using Pontryagin's Minimum Principle (PMP) is discussed in Section IV, highlighting the differences with respect to the traditional case in which the fuel consumption is the only minimization objective. The PMP can be implemented online as an adaptive equivalent consumption minimization strategy (ECMS). Section V presents simulation results to demonstrate the usefulness of this approach.

II. Battery aging

It is well known that the charge/discharge cycles undergone by electrochemical batteries tend to decrease their charge capacity and the amount of power they can deliver (by increasing the internal resistance). Many research papers are devoted to quantifying the loss of capacity/power during a battery's lifetime and its relation to the actual operating conditions [2], [3], [4], [5]. In fact, the battery in a vehicle operates under highly dynamic conditions that do not match the cycles traditionally used by the manufacturers to characterize the cycle life in laboratory conditions. A framework for phenomenological battery life estimation in electrified vehicles has been proposed in recent years by researchers at the Ohio State University [6], [7], [8], [9], and is briefly summarized in this section. It is based on a damage accumulation model that uses the concept of *accumulated Ah-throughput*, i.e. the total amount of electrical charge (in both charge and discharge) that can flow to and from the battery before this reaches the end of life. The accumulated Ah-throughput depends on the actual operating conditions: in fact, at the cell level, the severity of the charge transfer depends on the current severity relative to battery size (i.e., C-rate I_c), the operating temperature θ, and the depth of discharge $DOD = 1 - SOC$ [7]. The C-rate is an index defined as the ratio of the current (in A) to the nominal charge capacity (in Ah):

$$I_c = \frac{I \text{ [A]}}{Q_{batt} \text{ [Ah]}}. \tag{1}$$

In electric and hybrid vehicles, the quantity that is considered as the main indication of battery age is its charge capacity, and the generally accepted definition of end of life corresponds to the capacity reaching 80% of the original value [10].

Usually, battery manufacturers define battery life with respect to a nominal cycle with these characteristics: $I_c = 1$, $DOD = 100\%$, $\theta = 25°$C. The battery life Γ is defined as the total Ah-throughtput when the battery is subject to this nominal load cycle [8]:

$$\Gamma = \int_0^{EOL} |I_{nom}(t)|\, dt. \tag{2}$$

where $I_{nom}(t)$ is the nominal current and EOL indicates the battery end of life. For a given battery, the quantity Γ defined by (2) is constant.

In this paper, we characterize the aging effect of any cycle the battery undergoes with respect to the nominal cycle, using the concept of *severity factor,* σ. The severity factor of a given cycle (i.e. a set of values of current, temperature, SOC and DOD) is defined as

$$\sigma\left(I, \theta, SOC\right) = \frac{\gamma(I, \theta, SOC)}{\Gamma} = \frac{\int_0^{EOL} |I(t)|\, dt}{\int_0^{EOL} |I_{nom}(t)|\, dt} \tag{3}$$

where $\gamma(I, \theta, SOC)$ is the battery duration (Ah-throughput) corresponding to a given sequence of current, temperature,

L. Serrao and A. Sciarretta are with IFP Energies Nouvelles, 92852 Rueil-Malmaison (France). E-mail: {lorenzo.serrao, antonio.sciarretta}@ifpen.fr. S. Onori, Y. Guezennec and G. Rizzoni are with the Center for Automotive Research at The Ohio State University, Columbus, OH 43212 (US). E-mail: {onori.1, guezennec.1, rizzoni.1}@osu.edu.

and SOC; and Γ is the total Ah-throughput corresponding to the nominal cycle. The severity factor represents the relative aging effect with respect to the nominal cycle, and it is higher than 1 for conditions which are more severe in terms of aging (i.e. would bring to shorter life).

In order to compute the effective life depletion from the charge exchange, the *effective Ah-throughput* [9] is computed as

$$Ah_{eff}(t) = \int_0^t \sigma\left(I(\tau), \theta(\tau), SOC(\tau)\right) \cdot |I(\tau)|\, d\tau \quad (4)$$

which represents the amount of charge that would need to be exchanged using the nominal cycle to have the same aging effect as the actual cycle undergone by the battery. The condition of end of life is defined as the moment at which $Ah_{eff}(t) = \Gamma$. The quantity $Ah_{eff}(t)$ is the measure of the battery aging used in this paper and it is part of the cost function for our problem formulation in the form $\frac{Ah_{eff}}{\Gamma}$, which represents the fraction of life depleted during a driving cycle.

The concept of severity maps to express the relative aging effect of a cycle was proposed in [8], [9] specifically for the case of plug-in hybrid electric vehicles (PHEVs). In those vehicles, the battery charge capacity is quite large, to allow significant all-electric range. Thus, the C-rate tends to be fairly small and therefore its effect on aging is negligible. An example of a severity factor function depending on SOC and temperature is shown in [8]. The severity factor map as postulated in [8] originates from data available in literature for Li-ion phosphate battery cells. Experimental testing is currently undergoing at the Ohio State University Center for Automotive Research, in order to build such maps.

Following a similar approach, the severity factor map of Figure 1 is postulated in this paper. The map shown is a function of three parameters, and is represented here as a surface in the domain (SOC, I_c) parameterized in θ. Since the focus of this paper is on charge-sustaining HEVs (with smaller batteries than PHEVs), the effect of C-rate is not negligible anymore and is actually the most important aging factor. Another aspect specific to HEVs is the SOC range, less wide than in plug-in vehicles. The temperature effect is also important, as temperature above 25 °C makes aging faster. The map shows a region where $\sigma \approx 1$, corresponding to operating conditions that do not harm the battery more than the nominal cycle; and a region where, instead, the severity factor is much higher, indicating conditions that are very severe in terms of battery aging.

The map is only postulated and experimental data points are needed to validate it, especially in the regions with higher severity. However, it is believed to be a reasonable assumption for the purpose of this paper, which focuses on the methodology rather than the experimental results.

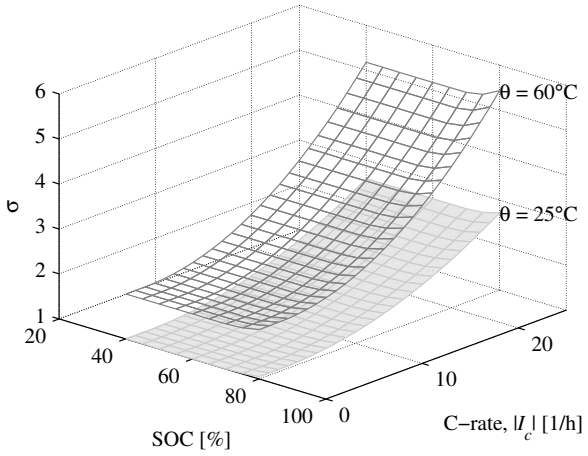

Fig. 1: Severity factor map used for the simulations

III. Problem formulation

The objective of the optimal control strategy is to minimize the overall cost during a trip. Unlike most preceding works on HEV optimization [1], in which the cost function is the fuel consumption, in this paper the cost includes both the fuel consumption and the fraction of battery life depleted:

$$J = \int_0^{t_f} (1-\alpha) \cdot \dot{m}_f\left(u(t), P_{req}(t)\right) + \alpha \cdot c_a \frac{1}{\Gamma} \sigma\left(I(u(t)), \theta(t), SOC(t)\right) \cdot |I(u(t))|\, dt \quad (5)$$

where $\dot{m}_f$ is the fuel consumption, $u(t) = P_{batt}(t)$ is the control variable, $P_{req}(t)$ the total power demand. c_a is a transformation coefficient of the battery wear, to make it dimensionally compatible with the fuel consumption, and α is a weighting factor to adjust the relative importance of the two cost contributions. α is arbitrary, while c_a has the meaning of a physical parameter. For instance, a meaningful value for c_a is obtained by expressing the two costs in terms of monetary expense: thus c_a is the ratio of the battery replacement cost to the cost of 1 kg of gasoline. The power split between the engine and the battery, denoted as $u(t)$, is the control variable for the problem. It determines univocally the battery current $I(t)$, given the instantaneous power request $P_{req}(t)$. In physical terms, the power split variable chosen here is the battery power. The total power demand $P_{req}(t)$ is an external input and its instantaneous value is assumed to be known at each time.

The system has two states: the temperature and the state of charge, both of which affect significantly battery aging. In this paper, the temperature variation is neglected, assuming a constant temperature: $\theta(t) = \theta_0$. The SOC is then the only dynamic state; its equation, derived using the circuit model

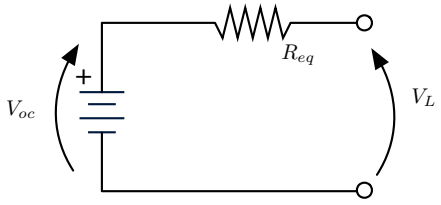

Fig. 2: Battery circuit model to derive (6)

of Figure 2, is[1]:

$$S\dot{O}C\left(P_{batt}, SOC, \theta\right) = -\frac{1}{Q_{batt}} I\left(P_{batt}, SOC, \theta\right) = \\ -\frac{V_{oc}(SOC) + \sqrt{V_{oc}^2(SOC) - 4 \cdot P_{batt} \cdot R_{eq}\left(SOC, \theta\right)}}{2 \cdot R_{eq}\left(SOC, \theta\right) \cdot Q_{batt}} \tag{6}$$

where Q_{batt} is the battery charge capacity, P_{batt} is the power at the battery terminals, $V_{oc}(SOC)$ the open-circuit voltage, and $R_{eq}\left(SOC, \theta\right)$ the equivalent internal resistance.

Adding the temperature as a second state and optimizing the temperature control may prove interesting in itself and practically valuable, but it adds complexity to the problem, resulting in an optimal control problem with two states (similar to what is proposed in [11]). In this paper, this aspect is not considered and instead focus is given to the effect of aging on the energy management. Investigating the effect of thermal management represents a further enhancement, which is object of current work.

IV. Analytical solution

Pontryagin's Minimum Principle (PMP) [12], [13] is applied to the problem in order to find an implementable optimal solution to the energy management problem [14], [15]. The principle states that the optimal control $u^*(t)$ minimizes at each instant the Hamiltonian function defined as follows

$$H\left(u, SOC, \theta, P_{req}, \lambda_{SOC}, \lambda_\theta\right) = \\ (1-\alpha)\cdot\dot{m}_f\left(u, P_{req}\right) + \alpha \cdot c_a \frac{1}{\Gamma}\sigma\left(I, \theta, SOC\right)\cdot\left|I\left(u, SOC, \theta\right)\right| \\ + \lambda_{SOC}(t)\cdot S\dot{O}C(u, SOC, \theta), \tag{7}$$

where the co-state variable $\lambda_{SOC}(t)$ evolves according to the following dynamic equations:

$$\dot{\lambda}_{SOC}(t) = -\frac{\partial H}{\partial SOC} = \alpha c_a \frac{1}{\Gamma}\frac{\partial \sigma\left(I, \theta, SOC\right)}{\partial SOC} \\ - \lambda_{SOC}(t)\frac{\partial S\dot{O}C\left(u, SOC, \theta\right)}{\partial SOC} \tag{8}$$

while the state variable $SOC(t)$ evolves according to (6).

The resulting systems of two differential equations has a known initial condition (initial SOC), and one final condition that is imposed (the SOC value desired at the end).

[1]To simplify the notation, from now on the time-dependence of $u(t)$, $SOC(t)$, $\theta(t)$ is not indicated explicitly when they are used as function arguments.

A. Case A: aging is not taken into account

If the weight of aging α is set to zero in the cost function (5) , the standard HEV energy management problem is found:

$$H\left(u, SOC, \theta, P_{req}, \lambda_{SOC}\right) = \\ \dot{m}_f\left(u, P_{req}\right) + \lambda_{SOC}(t)\cdot S\dot{O}C(u, SOC, \theta), \tag{9}$$

$$\dot{\lambda}_{SOC}(t) = -\frac{\partial H}{\partial SOC} = -\lambda_{SOC}(t)\frac{\partial S\dot{O}C\left(u, SOC, \theta\right)}{\partial SOC} \tag{10}$$

For a more intuitive representation [15], the Hamiltonian can be rewritten by introducing the *equivalence factor* $s(t) = \lambda_{SOC}(t) \cdot Q_{lhv}/E_{batt}$, which is a rescaling of $\lambda_{SOC}(t)$ to make it adimensional:

$$H\left(u, SOC, \theta, P_{req}, s\right) = \\ \dot{m}_f\left(u, P_{req}\right) + s(t) \cdot \frac{E_{batt}}{Q_{lhv}}\cdot S\dot{O}C(u, SOC, \theta), \tag{11}$$

where E_{batt} is the battery total energy and Q_{lhv} the fuel lower heating value (i.e. its specific energy). Eq. (11) can be seen as an equivalent fuel consumption in which the term $s(t)\cdot\frac{E_{batt}}{Q_{lhv}}\cdot S\dot{O}C(u, SOC, \theta)$ represents the fuel consumption equivalent to the charge/discharge of the battery.

Since the equivalence factor is proportional to the co-state $\lambda_{SOC}(t)$, its variation is also given by a rescaling of (10):

$$\dot{s}(t) = -\frac{Q_{lhv}}{E_{batt}} \cdot \dot{\lambda}_{SOC}(t) = -s(t)\frac{\partial S\dot{O}C\left(u, SOC, \theta\right)}{\partial SOC}. \tag{12}$$

Thus, the control at each instant is given by

$$u^*(t) = \arg\min H\left(u, SOC, \theta, P_{req}, s\right), \tag{13}$$

with

$$SOC(t) = SOC(0) - \frac{1}{Q_{batt}}\int_0^t I(SOC, \theta, u)d\tau \tag{14}$$

and

$$s(t) = s_0 - \int_0^t s(\tau)\frac{\partial S\dot{O}C\left(u, SOC, \theta\right)}{\partial SOC}d\tau. \tag{15}$$

While the initial value of state of charge is given, the initial value s_0 of the equivalence factor is not known a-priori. Instead, it is known the final value of the state, which should be

$$SOC(t_f) = SOC_{target}. \tag{16}$$

For a given driving cycle, there exists only one initial value of the equivalence factor for which the solution that minimizes (11) at each time is also such that the terminal condition $SOC(t_f) = SOC_f$ is satisfied [15], [16]; this corresponds to the optimal solution to the problem.

In the case of offline optimization, in order to obtain a solution that meets both terminal conditions on SOC, a dichotic search is used to determine the initial value $s(0) = s_0$

of the equivalence factor that generates the correct final value $SOC(t_f)$ [15], [16]; for online implementation, instead, the equivalence factor is changed dynamically using feedback of the state of charge. For example, the method proposed in [17] recognizes the fact that the effect of the initial value $s(0)$ affects the behavior during the entire optimization horizon; thus, the overall horizon is divided into smaller sections and the initial value is modified at the beginning of each section using SOC feedback, in order to reach the desired SOC_{target} after several sections.

B. Case B: aging is taken into account

In this case the cost of aging is taken into account (i.e. $\alpha \neq 0$). The Hamiltonian (7) becomes

$$\begin{aligned} &H\left(u, SOC, \theta, P_{req}, \lambda_{SOC}\right) = \\ &\quad (1-\alpha)\cdot \dot{m}_f\left(u, P_{req}\right) + \lambda_{SOC}(t)\cdot \dot{SOC}\left(u, SOC, \theta\right) \\ &\qquad + \alpha \cdot c_a \frac{1}{\Gamma}\sigma\left(I, \theta, SOC\right)\cdot \left|I\left(u, SOC, \theta\right)\right| \end{aligned} \quad (17)$$

and the co-state variation is given by

$$\begin{aligned} &\dot{\lambda}_{SOC}(t) = -\frac{\partial H}{\partial SOC} = \\ &-\alpha\cdot c_a \frac{1}{\Gamma}\frac{\partial \sigma\left(I, \theta, SOC\right)}{\partial SOC} - \lambda_{SOC}(t)\frac{\partial \dot{SOC}\left(u, SOC, \theta\right)}{\partial SOC}. \end{aligned} \quad (18)$$

These equations can be written in terms of equivalent fuel consumption and equivalence factor:

$$\begin{aligned} &H\left(u, SOC, \theta, P_{req}, s\right) = \\ &(1-\alpha)\cdot \dot{m}_f\left(u, P_{req}\right) + s(t)\cdot \frac{E_{batt}}{Q_{lhv}}\cdot \dot{SOC}(u, SOC, \theta) \\ &\qquad + \alpha \cdot c_a \frac{1}{\Gamma}\sigma\left(I, \theta, SOC\right)\cdot \left|I\left(u, SOC, \theta\right)\right| \end{aligned} \quad (19)$$

$$\dot{s}(t) = -s(t)\frac{\partial \dot{SOC}\left(u, SOC, \theta\right)}{\partial SOC} - \alpha \frac{Q_{lhv}}{E_{batt}} c_a \frac{1}{\Gamma}\frac{\partial \sigma\left(I, \theta, SOC\right)}{\partial SOC} \quad (20)$$

In (19), the three terms represents respectively the cost of using the engine (fuel consumption), the cost of using the battery in terms of energy (discharge or charge), and the cost in terms of battery life depletion. A parallel with the previous approach described in Section IV-A can be drawn. The first two terms are the same in both cases, and their sum is interpreted as an equivalent fuel consumption accounting for battery charge/discharge, as described in Section IV-A. However, in this case an additional term is present, accounting for the aging effect of a given control action: it can be seen as the fuel consumption equivalent of the battery life depletion. In addition to this direct influence of aging on the instantaneous cost, the variation of the equivalence factor $s(t)$ also depends on the aging effect, because of the term $\frac{\partial \sigma(I,\theta,SOC)}{\partial SOC}$ in (20). In keeping with the ECMS interpretation, this means that even the cost of battery *energy* is affected by the shape of the severity factor surface, increasing when a SOC variation makes more intense the aging effect on the battery. The term $\frac{\partial \sigma(I,\theta,SOC)}{\partial SOC}$ is obtained as the numerical gradient of the surface shown in Figure 1.

The solution is still given by (13) and (14), which remain the same, while (15) becomes

$$\begin{aligned} s(t) = s_0 &- \int_0^t s(\tau)\frac{\partial \dot{SOC}\left(u, SOC, \theta\right)}{\partial SOC} d\tau \\ &- \int_0^t \alpha \frac{Q_{lhv}}{E_{batt}} c_a \frac{1}{\Gamma}\frac{\partial \sigma\left(I, \theta, SOC\right)}{\partial SOC} d\tau. \end{aligned} \quad (21)$$

Again, like in the previous case, the behavior of the solution depends on the initial value of the equivalence factor, s_0. Note that, formally, case B is identical to case A when $\alpha = 0$.

TABLE I: Vehicle characteristics

Vehicle mass	1800 kg
Engine max. power	100 kW
Motor max. power	25 kW
Battery energy capacity	1 kWh (3600 kJ)
Battery Ah life (nominal cycle), Γ	20000 Ah

TABLE II: Cost assumptions for two examples. Battery replacement cost is estimated for a 1-kWh Li-Ion battery, for the final customer. Cost of gasoline observed in April 2011.

	Battery cost	Gasoline cost	c_a [kg]
Europe	2000 €	1.5 €/l = 2.1 €/kg	~950
USA	3000 $	3.5 $/gal = 1.3 $/kg	~2300

V. Simulation results

Simulations are ran using a quasi-static model for vehicle longitudinal dynamics and powertrain energy flows, implemented using look-up tables for computing fuel consumption and battery power. The vehicle considered is a mid-size sedan with a parallel hybrid powertrain, whose characteristics are listed in Table I.

The cost of battery life is $c_a = \frac{c_{batt}}{c_{fuel}}$ where c_{batt} is the cost of battery replacement, and c_{fuel} is the cost of 1 kg of fuel. Orders of magnitude for the numerical values are reported in Table II. Since the focus of this paper is not on economic evaluation, these values are intended only to generate an estimate of c_a, which is set to 950kg for the simulations in this paper.

The two approaches described in Sections (IV-A) (no aging) and (IV-B) (with aging) are compared here, considering offline optimization of the value s_0. The variation of the equivalence factor $s(t)$ is given by either (15) or (21) in the two approaches respectively.

The battery depletion is computed using directly (4), where the severity factor is obtained by interpolation of the surface in Figure 1, and the derivative $\frac{\partial \sigma}{\partial SOC}$ is computed taking the numerical gradient of the surface.

The results on a cycle composed by the Artemis urban and suburban cycle are shown in Figure 3. The cases $\alpha = 0$, $\alpha = 0.35$, and $\alpha = 0.5$ are shown. The first represents

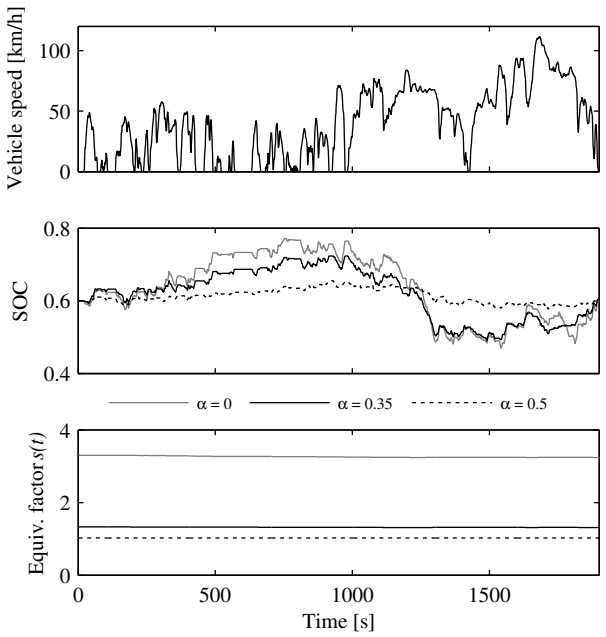

Fig. 3: Comparison of the solutions obtained with and without accounting for the aging effect in the cost function.

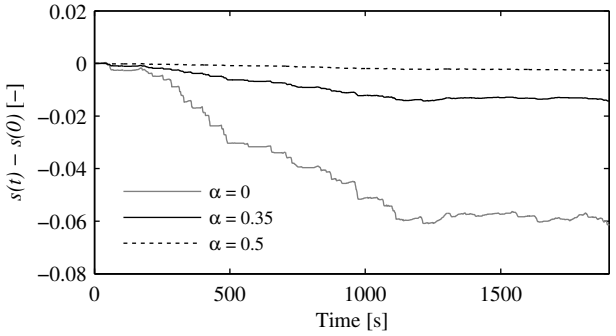

Fig. 4: Variation during the driving cycle of the equivalence factor given by (20) for the three cases of Figure 3.

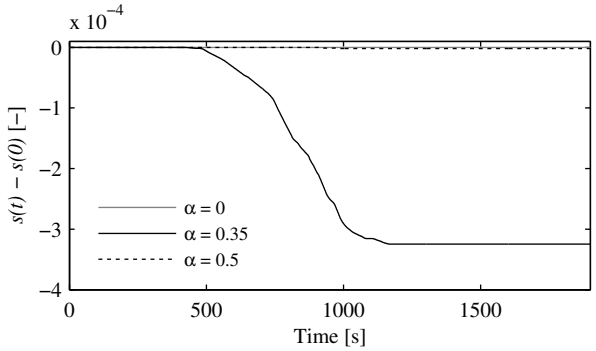

Fig. 5: Contribution of aging to the equivalence factor variation of Figure 4, as given by the second term of (20).

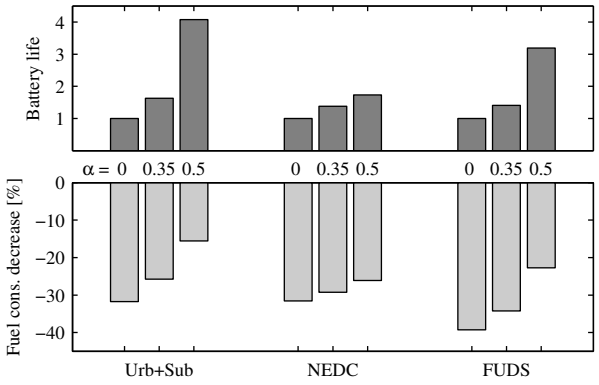

Fig. 6: Variation in fuel consumption and battery life depletion for several driving cycles and values of α. The fuel consumption is expressed as reduction with respect to the conventional vehicle (no hybridization). The battery life is normalized with respect to the case $\alpha = 0$.

the approach A, while the latter are two instances of case B. A difference in the SOC evolution is evident between the three cases: in particular, the solutions that account for battery aging ($\alpha > 0$) tend to keep the SOC in a different range, corresponding to less harmful conditions for the battery, while the case $\alpha = 0$ tends to use the battery more aggressively. The equivalence factor changes significantly between the three cases. In fact, s represents the weight of the battery power with respect to the rest of the Hamiltonian, and adding battery aging to the two original elements of the Hamiltonian function (fuel consumption and battery power) changes the balance among the terms.

The dynamic variation of $s(t)$, instead, is very small in all cases, so much that it is invisible in Figure 3. The variation alone (with respect to the initial value) is shown in Figure 4. It remains essentially related to the SOC variation, since the contribution of aging, visible in Figure 5, is 2 or 3 orders of magnitude smaller than the overall variation.

The fuel consumption and battery expected life are reported in Figure 6, which shows this cycle (denoted as *Urb+Sub*) together with other regulatory driving cycles. From the bar plot, it is clear how accounting for battery aging has a significant impact on the battery lifetime depleted during the trip, but this introduces a tradeoff with fuel consumption, which increases, since the battery is used to a minor extent. The tradeoff point depends on the value of the parameter α, which weighs the increase in battery life and the penalization in fuel consumption.

For a visual justification of the differences in terms of aging, Figure 7 shows the operating points corresponding the three cases on the severity factor map: it can be seen how the strategies that account for battery aging operate in a narrower range of state of charge and current, to ensure lower values of the severity factor.

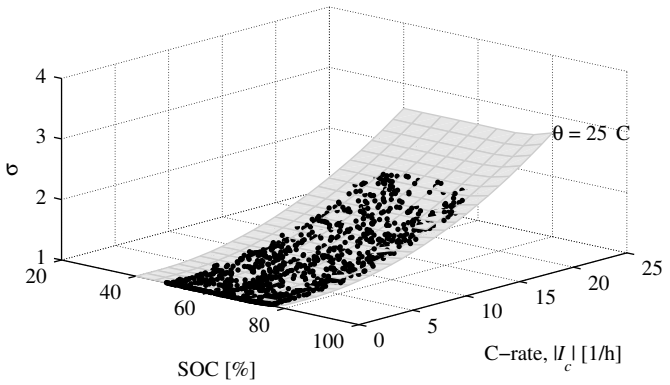

(a) $\alpha = 0$

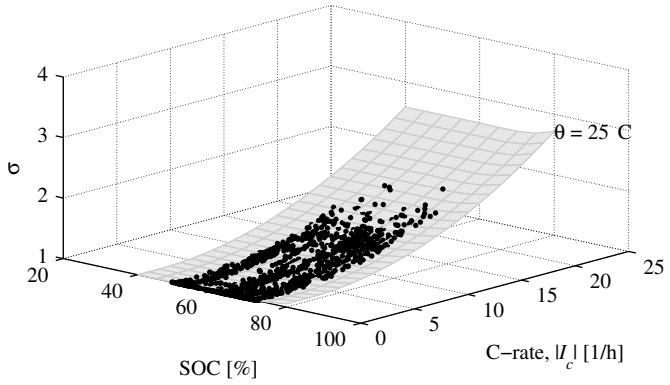

(b) $\alpha = 0.35$

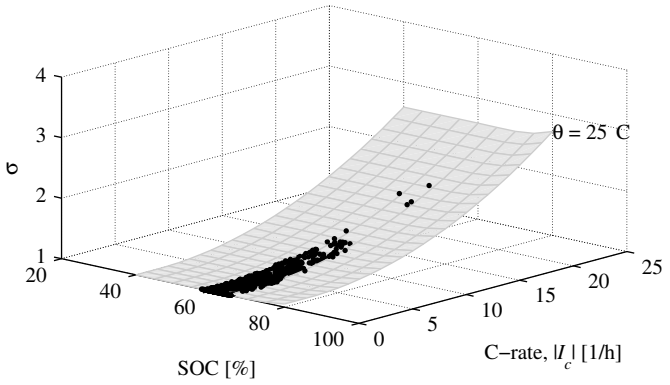

(c) $\alpha = 0.50$

Fig. 7: Distribution of the operating points on the severity factor map, for the three cases compared in Figure 3

CONCLUSION

A generic approach to take into account battery aging in energy management strategies is proposed in this paper, using recently developed approaches to battery lifetime estimation. While the results obtained are based a postulated map of the severity factor, still to be verified experimentally, the approach has the potentiality to account quantitavely for battery aging in the context of energy management strategies. The results will depend strongly on the quality of aging characterization for the batteries used, and introduce a compromise between the performance (fuel consumption) and the battery lifetime. Ongoing reseach focuses on experimental validation of the severity factor map, and on the introduction of thermal dynamics in the optimization problem.

REFERENCES

[1] A. Sciarretta and L. Guzzella, "Control of hybrid electric vehicles," *IEEE Control Systems Magazine*, pp. 60–70, April 2007.

[2] H. Wenzl, I. Baring-Gould, R. Kaiser, B. Liaw, P. Lundsager, J. Manwell, A. Ruddell, and V. Svoboda, "Life prediction of batteries for selecting the technically most suitable and cost effective battery," *Journal of Power Sources*, vol. 144, no. 2, pp. 373–384, 2005.

[3] P. Rong and M. Pedram, "An analytical model for predicting the remaining battery capacity of lithium-ion batteries," *Very Large Scale Integration (VLSI) Systems, IEEE Transactions on*, vol. 14, no. 5, pp. 441–451, 2006.

[4] K. Smith, C. Rahn, and C. Wang, "Model-based electrochemical estimation and constraint management for pulse operation of lithium ion batteries," *IEEE Transactions on Control Systems Technology*, vol. 18, no. 3, pp. 654 – 663, 2008.

[5] D. U. Sauer and H. Wenzl, "Comparison of different approaches for lifetime prediction of electrochemical systems–using lead-acid batteries as example," *Journal of Power Sources*, vol. 176, no. 2, pp. 534 – 546, 2008.

[6] L. Serrao, Z. Chehab, Y. Guezennec, and G. Rizzoni, "An aging model of Ni-MH batteries for hybrid electric vehicles," *Proceedings of the 2005 IEEE Vehicle Power and Propulsion Conference (VPP05)*, pp. 78–85, 2005.

[7] L. Serrao, S. Onori, G. Rizzoni, and Y. Guezennec, "A novel model-based algorithm for battery prognosis," *Proceeding of the 7th IFAC Symposium on Fault Detection, Supervision and Safety of Technical Processes (SAFEPROCESS 09)*, 2009.

[8] V. Marano, S. Onori, N. Madella, Y. Guezennec, and G. Rizzoni, "Lithium-ion batteries life estimation for plug-in hybrid electric vehicles," *Proceedings of the 2009 IEEE Vehicle Power and Propulsion Conference (VPP09)*, 2009.

[9] A. Di Filippi, S. Stockar, S. Onori, M. Canova, and Y. Guezennec, "Model-based life estimation of li-ion batteries in phevs using large scale vehicle simulations," *Proceedings of the 2010 IEEE Vehicle Power and Propulsion Conference (VPP10)*, 2010.

[10] IEEE SCC 29, "IEEE 485-1997, recommended practice for sizing lead-acid batteries for staionary applications," 1997.

[11] J. Lescot, A. Sciarretta, Y. Chamaillard, and A. Charlet, "On the integration of optimal energy management and thermal management of hybrid electric vehicles," *Proceedings of the 2010 IEEE Vehicle Power and Propulsion Conference (VPPC10)*, 2010.

[12] H. P. Geering, *Optimal Control with Engineering Applications*. Berlin Heidelberg: Springer, 2007.

[13] D. S. Naidu, *Optimal Control Systems*. Boca Raton, FL: CRC Press, 2003.

[14] A. Chasse, G. Hafidi, P. Pognant-Gros, and A. Sciarretta, "Supervisory control of hybrid powertrains: an experimental benchmark of offline optimization ond online energy management," *Proceeding of the IFAC Workshop on Engine and Powertrain Control, Simulation and Modeling (E-COSM)*, 2009, and *Control Engineering Practice (accepted for publication)*, 2011.

[15] L. Serrao, S. Onori, and G. Rizzoni, "ECMS as a Realization of Pontryagin's Minimum Principle for HEV Control," *Proceedings of the 2009 American Control Conference*, 2009.

[16] A. Chasse, A. Sciarretta, and J. Chauvin, "Online optimal control of a parallel hybrid with costate adaptation," *Proceedings of the 6th IFAC Symposium "Advances in Automotive Control"*, 2010.

[17] S. Onori, L. Serrao, and G. Rizzoni, "Adaptive equivalent consumption minimization strategy for hybrid electric vehicles," *Proceedings of the 2010 ASME Dynamic Systems and Control Conference*, 2010.